applied sciences

MDPI

Article

Exploratory Analysis of Differentially Expressed Genes for Distinguishing Adipose-Derived Mesenchymal Stroma/Stem Cells from Fibroblasts

Masami Kanawa [1,*], Katsumi Fujimoto [2], Tania Saskianti [3], Ayumu Nakashima [4,5] and Takeshi Kawamoto [1,6]

[1] Natural Science Center for Basic Research and Development, Hiroshima University, Hiroshima 734-8533, Japan; tkawamo@hiroshima-u.ac.jp
[2] Department of Molecular Biology and Biochemistry, Graduate School of Biomedical and Health Sciences, Hiroshima University, Hiroshima 734-8533, Japan; kfujimo@hiroshima-u.ac.jp
[3] Department of Pediatric Dentistry, Faculty of Dental Medicine, Universitas Airlangga, Surabaya 60132, Indonesia; tania-s@fkg.unair.ac.id
[4] Department of Stem Cell Biology and Medicine, Graduate School of Biomedical and Health Sciences, Hiroshima University, Hiroshima 734-8533, Japan; ayumu@hiroshima-u.ac.jp
[5] Department of Nephrology, Graduate School of Medicine, University of Yamanashi, Yamanashi 409-3898, Japan
[6] Writing Center, Hiroshima University, Higashi-Hiroshima 739-8512, Japan
* Correspondence: mfuku@hiroshima-u.ac.jp; Tel.: +81-82-257-1601

Abstract

Adipose-derived mesenchymal stromal/stem cells (AT-MSCs) can be typically isolated from adipose tissue using a minimally invasive procedure. However, since AT-MSCs are usually obtained from subcutaneous tissue, there is a risk of contamination with fibroblasts (FBs), which can reduce the differentiation potential of AT-MSCs. To avoid this contamination, it is crucial to identify specific markers to effectively distinguish AT-MSCs from FBs. Analysis of microarray data obtained from three studies (GSE9451, GSE66084, GSE94667, and GSE38947) revealed 123 genes expressed at levels more than 1.5-fold higher in AT-MSCs compared to FBs. Using STRING, a protein-protein interaction (PPI) network consisting of 80 nodes and 197 edges was identified within the 123 genes. Further investigation using Molecular Complex Detection in Cytoscape identified a module of 12 genes: *COL3A1*, *FBN1*, *COL4A1*, *COL5A2*, *POSTN*, *CTGF*, *SPARC*, *HSPG2*, *FSTL1*, *LAMA2*, *LAMC1*, *COL16A1*. Gene Ontology analysis revealed that these genes were enriched in extracellular region (GO: 0005576). Additionally, these 12 genes corresponded to the top 12 of the 15 hub genes calculated using the Maximal Clique Centrality algorithm. The results of this study suggest that these 12 genes may serve as markers for distinguishing AT-MSCs from FBs, offering potential applications in regenerative medicine.

Keywords: adipose-derived mesenchymal stem cells; gene markers; extracellular matrix; fibroblasts; hub genes; protein-protein interaction (PPI) network

check for updates

Academic Editor: Gang Wei

Received: 12 August 2025
Revised: 3 September 2025
Accepted: 8 September 2025
Published: 9 September 2025

Citation: Kanawa, M.; Fujimoto, K.; Saskianti, T.; Nakashima, A.; Kawamoto, T. Exploratory Analysis of Differentially Expressed Genes for Distinguishing Adipose-Derived Mesenchymal Stroma/Stem Cells from Fibroblasts. *Appl. Sci.* **2025**, *15*, 9881. https://doi.org/10.3390/app15189881

Copyright: © 2025 by the authors. Licensee MDPI, Basel, Switzerland. This article is an open access article distributed under the terms and conditions of the Creative Commons Attribution (CC BY) license (https://creativecommons.org/licenses/by/4.0/).

1. Introduction

Mesenchymal stromal/stem cells (MSCs), which can differentiate into multiple cell types such as osteocytes, chondrocytes, adipocytes, myocytes, and nerve cells [1–3], have garnered considerable attention in recent years as promising sources for regenerative medicine. MSCs can be isolated from various tissues, including bone marrow, placenta,

umbilical cord blood, synovium, dental pulp, and adipose tissue [1,4–7]. Subcutaneous adipose tissue is a readily accessible source for obtaining substantial quantities of adipose-derived MSCs (AT-MSCs) through a minimally invasive procedure [8]. However, since adipose tissue is isolated from subcutaneous tissue, a risk of contamination with fibroblasts (FBs) exists [9]. MSCs are morphologically indistinguishable from FBs. These cells share similar surface immunophenotype and proliferation potential, although FBs have little differentiation capacities [10]. Contamination of MSC cultures with fibroblasts has been reported to impair therapeutic efficacy; the presence of fibroblasts as a cell contaminant in the MSC preparation abolished therapeutic effects of stem cell transplantation [11]. Therefore, the identification of reliable biomarkers to distinguish AT-MSCs from FBs is essential to ensure the purity of MSC preparations and to safeguard the clinical effectiveness of MSC-based therapies.

Differences between MSCs and FBs are not fully understood. The International Society for Cellular Therapy defines MSCs as positive for the MSC markers CD105, CD73, and CD90, and negative for hematopoietic lineage markers [12]. Recently, Alt et al. compared the surface antigen markers of AT-MSCs and FBs and found that the MSC markers CD44, CD73, and CD105 were positive in both AT-MSCs and FBs, whereas the endothelial cell marker CD31 and hematopoietic lineage markers CD14 and CD45 were negative in both cell types [13]. Zanata et al. also reported that AT-MSCs and FBs showed similar immunophenotypic profiles [14]. These findings suggest that distinguishing between AT-MSCs and FBs based on surface antigen differences is challenging.

Bioinformatics analysis of differentially expressed genes (DEGs) using a protein-protein interaction (PPI) network has recently been used to identify accurate and reliable markers. For example, in studies of various cancers, such as hepatocellular carcinoma, colorectal cancer, breast cancer, gastric cancer, and glioblastoma, PPI network analysis of DEGs has led to the identification of gene markers for diagnosis and prognosis [15–19]. In addition, similar approaches have been used to identify key genes involved in the osteogenic and chondrogenic differentiation of MSCs [20,21]. However, no studies have yet analyzed the differences between MSCs and FBs using PPI network analysis.

In a previous study, we analyzed the difference in gene expression between bone marrow-derived MSCs (BM-MSCs) and FBs using DNA microarray analysis and identified several DEGs that could serve as gene markers to distinguish BM-MSCs from FBs [22]. However, whether these markers can distinguish AT-MSCs from FBs remains unexplored.

In this study, we identified 123 DEGs that were expressed at >1.5-fold higher levels in AT-MSCs than in FBs by comparing microarray data. Using STRING and MCODE in Cytoscape (v3.10.3), we identified 80 nodes and 197 edges along with a module consisting of 12 genes within the PPI networks of the 123 DEGs. Gene Ontology (GO) analysis revealed that the 12 genes were enriched in the extracellular region of the cellular component (CC). Our findings suggest that the 12 genes comprising the module identified may serve as markers for distinguishing AT-MSCs from FBs.

2. Materials and Methods

2.1. Sample Collection

Microarray data for AT-MSCs, BM-MSCs, and FBs were obtained from three studies (Table 1). Gene expression profiles (GSE9451 [23,24], GSE66084 [24], GSE94667 [25], and GSE38947 [26]) were downloaded from the Gene Expression Omnibus (https://www.ncbi.nlm.nih.gov/geo/, accessed on 5 September 2025). The GSE9451 and GSE66084 microarray datasets were based on the GPL574 platform (Affymetrix Human Genome U133 Plus 2.0Array) (Affymetrix, Inc., Santa Clara, CA, USA). The GSE94667 dataset was based on the GPL16043 platform (GeneChip® PrimeView Human Gene Expression Array) (Affymetrix,

Inc.). The GSE38947 dataset was based on the GPL14550 platform (Agilent-028004 SurePrint G3 Human GE 8 × 60 K Microarray) (Agilent Technologies, Santa Clara, CA, USA). These datasets contained nine samples each of AT-MSCs, BM-MSCs, and FBs.

Table 1. Microarray datasets used in this study.

Study	Acronym	Source Name	GEO Series	GEO Sample	Donor No.
Study-A	AT-MSCs	adipose tissue mesenchymal stem cells	GSE66084	GSM1614057	1
	AT-MSCs	adipose tissue mesenchymal stem cells		GSM1614056	2
	AT-MSCs	adipose tissue mesenchymal stem cells		GSM1614058	3
	BM-MSCs	iliac mesenchymal stem cells	GSE9451	GSM239713	4
	BM-MSCs	iliac mesenchymal stem cells		GSM239715	5
	BM-MSCs	iliac mesenchymal stem cells		GSM239722	6
	FBs	skin fibroblasts		GSM239766	7
	FBs	skin fibroblasts		GSM239769	8
	FBs	gingival fibroblasts		GSM239801	9
Study-B	AT-MSCs	Adipose-derived mesenchymal stem cells	GSE94667	GSM2480568	10
	AT-MSCs	Adipose-derived mesenchymal stem cells		GSM2480567	11
	AT-MSCs	Adipose-derived mesenchymal stem cells		GSM2480569	12
	BM-MSCs	Bone marrow-derived mesenchymal stem cells		GSM2480556	13
	BM-MSCs	Bone marrow-derived mesenchymal stem cells		GSM2480555	14
	BM-MSCs	Bone marrow-derived mesenchymal stem cells		GSM2480557	15
	FBs	neonatal dermal fibroblasts		GSM2480544	16
	FBs	neonatal dermal fibroblasts		GSM2480545	17
	FBs	neonatal dermal fibroblasts		GSM2480546	18
Study-C	AT-MSCs	adipose stromal cells	GSE38947	GSM952620	19
	AT-MSCs	adipose stromal cells		GSM952621	20
	AT-MSCs	adipose stromal cells		GSM952622	21
	BM-MSCs	bone marrow mesenchymal stem cells		GSM952617	22
	BM-MSCs	bone marrow mesenchymal stem cells		GSM952619	23
	BM-MSCs	bone marrow mesenchymal stem cells		GSM952618	24
	FBs	foreskin fibroblasts		GSM952623	25
	FBs	foreskin fibroblasts		GSM952624	26
	FBs	foreskin fibroblasts		GSM952625	27

GEO: Gene Expression Omnibus.

2.2. Analysis of Gene Expression Patterns and Identification of DEGs

A unified standardized expression set of 7616 genes was created from cross-platform expression data of all 27 samples on the Subio platform (Subio, Inc., Kagoshima, Japan). To identify gene expression patterns across different cell types, hierarchical clustering was performed using Pearson's correlation. DEGs with higher expression in AT-MSCs than in FBs were screened, using an adjusted p value < 0.05 and fold change > 1.5 as cut-off criteria (Supplementary Table S1).

2.3. PPI Network and GO Analysis

The PPI network of DEGs was constructed by using the STRING online database (version 12.0) (https://string-db.org/) [27,28]. Interactions with a combined score > 0.4 were considered statistically significant. The constructed PPI network was then imported into Cytoscape (version 3.7.1) to visualize the molecular interaction networks [29]. The most significant module was identified using the plugin Molecular Complex Detection (MCODE) (version 1.5.1) [30], with the following selection criteria: MCODE score > 5, degree cutoff = 2, node score cutoff = 0.2, maximum depth = 100, and k-score = 2. Hub genes were calculated based on the Maximal Clique Centrality (MCC) algorithm [31] using the Cytoscape plugin CytoHubba (version 0.1). GO analysis was performed using g:Profiler (version e109_eg56_p17_773ec798) [32] (Supplementary Table S2).

3. Results

3.1. Hierarchical Clustering Analysis

The DNA microarray data of 27 samples (9 AT-MSCs, 9 BM-MSCs, and 9 FBs) were extracted from three studies (Table 1), and a standardized expression set of 7616 genes was created using the Subio platform. The 7616 genes were successfully categorized into three cell types, AT-MSCs, BM-MSCs, and FBs, using hierarchical clustering analysis (Figure 1). Six distinct clusters were identified: Cluster 1 consisted mainly of genes expressed at high levels in BM-MSCs but not in AT-MSCs and FBs. Cluster 2 contained genes expressed at high levels in FBs, but not in AT-MSCs and BM-MSCs. Cluster 3 consisted of genes expressed at low levels in AT-MSCs but not in BM-MSCs and FBs, whereas clusters 4a, 4b, and 4c contained genes expressed at high levels in AT-MSCs but not in BM-MSCs and FBs. Cluster 5 primarily comprised genes expressed at low levels in FBs, but not in AT-MSCs and BM-MSCs. Cluster 6 consisted of genes expressed at low levels in BM-MSCs but not in AT-MSCs and FBs.

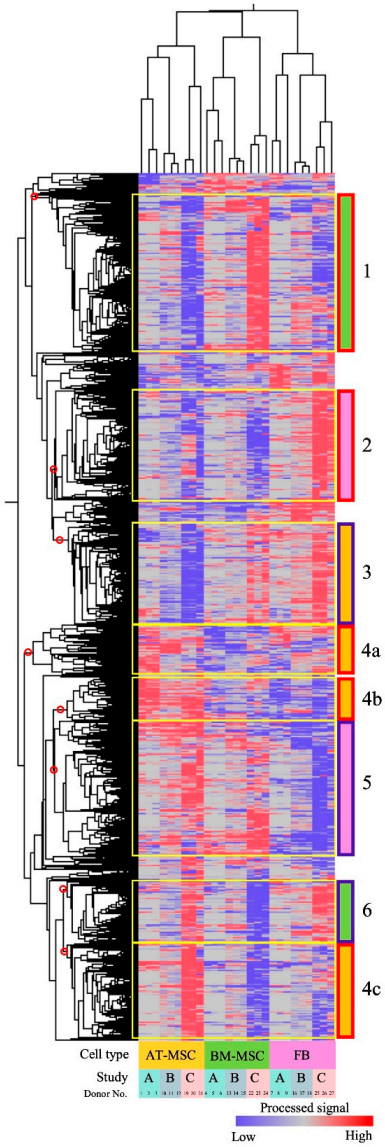


Figure 1. Heat map of hierarchical clustering of 7616 genes from AT-MSCs, BM-MSCs, and FBs. Each column represents a sample, and each row represents a gene. Dendrograms at the top and to the left show the relatedness of expression patterns for individual samples and individual probe sets (genes), respectively. Red circles mark identified clustering nodes. Expression pattern grouping is shown on the right of the heat map.

3.2. DEG Selection Between AT-MSCs and FBs and Construction of PPI Networks

Next, we sought to identify the DEGs between AT-MSCs and FBs. From the three studies, DEGs expressed at >1.5-fold higher levels in AT-MSCs than in FBs were selected. Using volcano plots, 685 DEGs in Study A, 904 DEGs in Study B, and 1565 DEGs in Study C were identified (Figure 2a). As shown in Figure 2b, the three studies shared 123 DEGs (Supplementary Table S1).

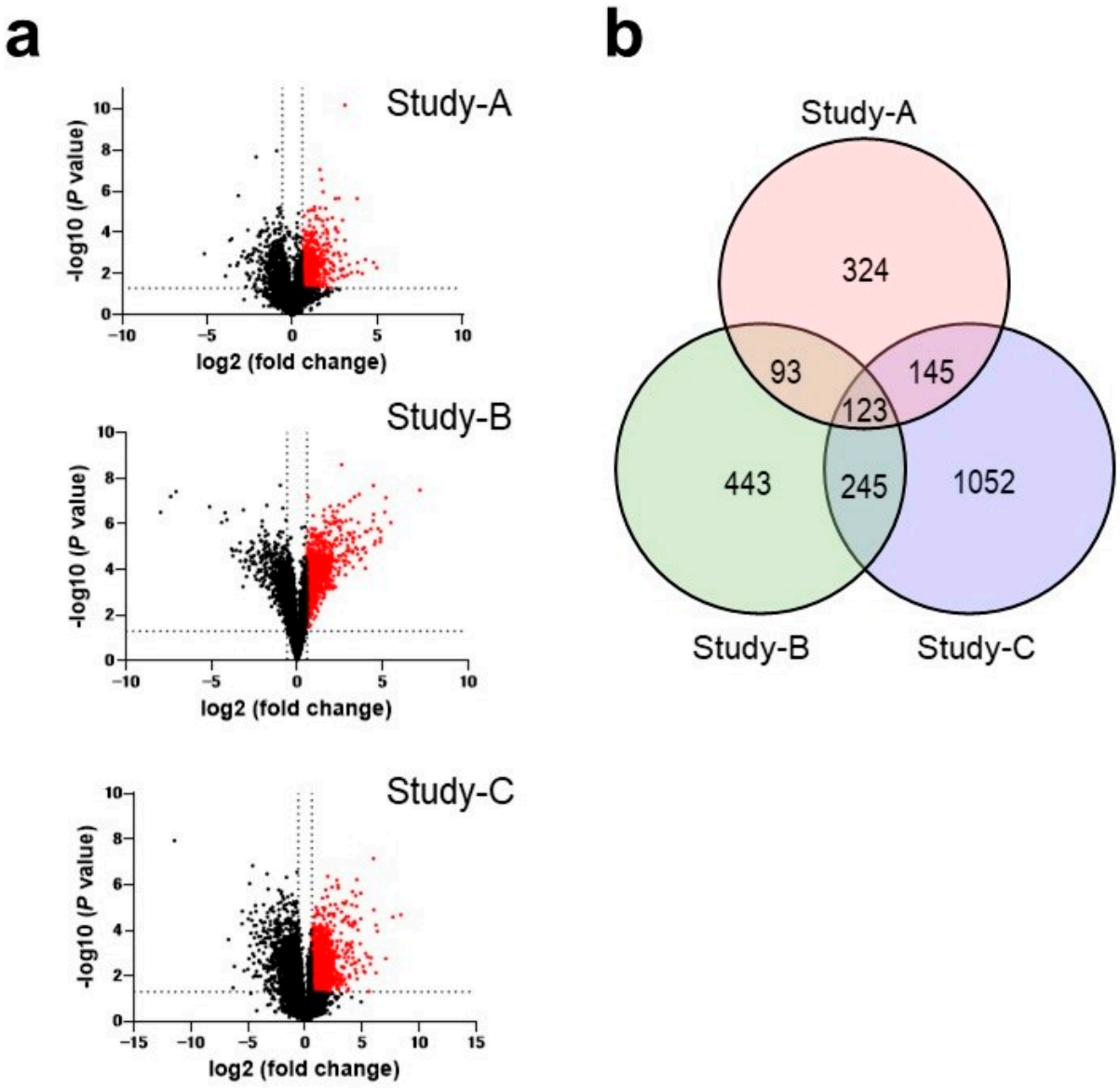


Figure 2. Identification of differentially expressed genes (DEGs) from three studies. (**a**) Volcano plots of the three studies. Red plots represent DEGs expressed at higher levels in AT-MSCs than in FBs with the criteria of p value < 0.05 and fold change > 1.5. (**b**) Venn diagram showing the overlap in the number of DEGs among three studies.

The list of 123 DEGs was uploaded to STRING in order to construct the PPI networks. A PPI network containing 80 nodes and 197 edges was identified (Figure 3a). Furthermore, using MCODE in Cytoscape, a significant module (Module A) with 12 nodes and 55 edges was identified (Figure 3b). The 12 nodes represented the following genes: *COL3A1*, *FBN1*, *COL4A1*, *COL5A2*, *POSTN*, *CTGF*, *SPARC*, *HSPG2*, *FSTL1*, *LAMA2*, *LAMC1*, and *COL16A1*.

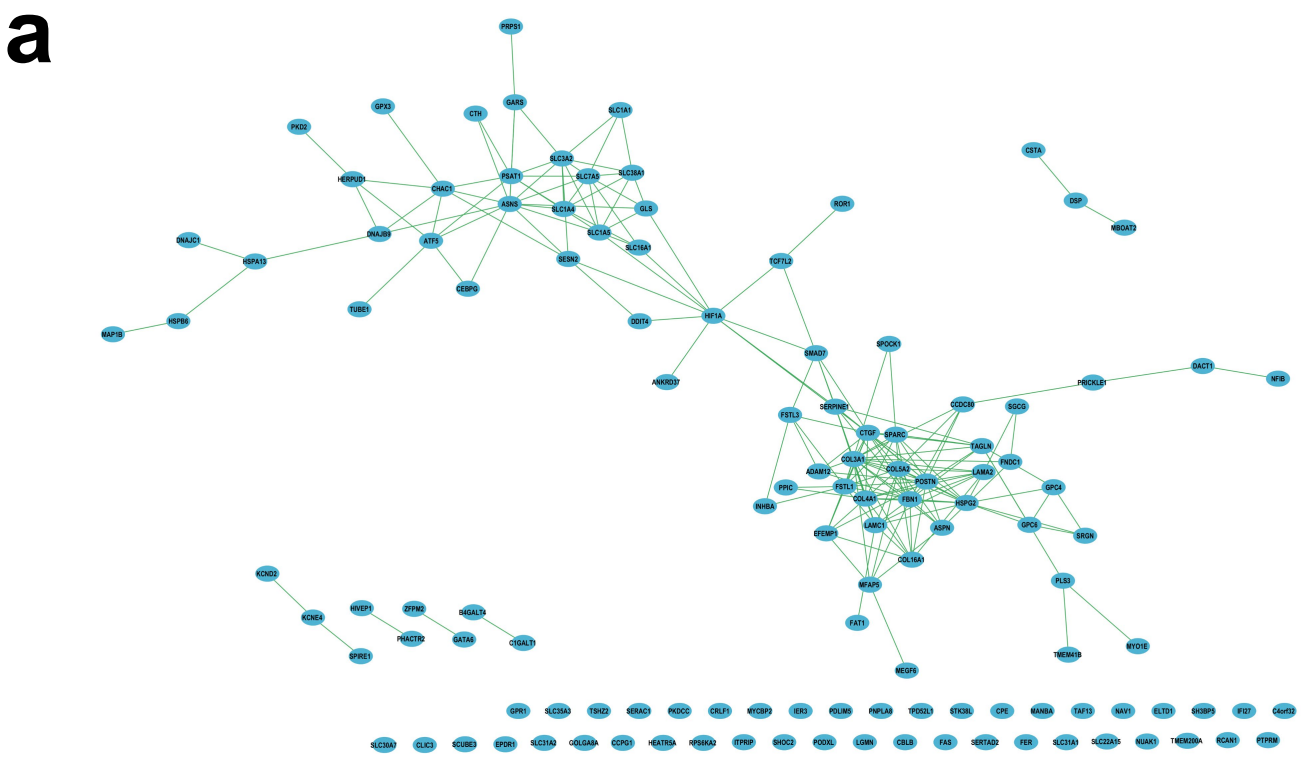


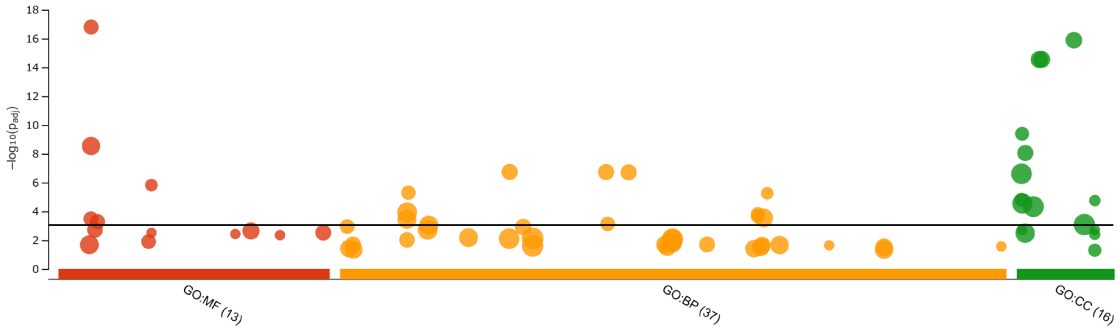
Figure 3. Identification of the module genes. (**a**) PPI network of 123 genes constructed by Cytoscape. (**b**) The identified module with 12 nodes and 55 edges (Module A).

3.3. GO Analysis

To investigate the functions of the 12 identified genes, we performed GO analysis using g:Profiler. We identified 13 molecular function (MF), 37 biological process (BP), and 16 CC terms for the 12 genes ($p < 0.05$) (Figure 4a and Supplementary Table S2). Notably,

all 12 genes were enriched in the extracellular region (GO: 0005576) of the CC (Figure 4b). Additionally, most of the genes were enriched in three key terms: extracellular matrix structural constituent (GO: 0005201) of MF, collagen-containing extracellular matrix (GO: 0062023) of CC, and extracellular matrix (GO: 0031012) of CC. Furthermore, *COL3A1*, *COL16A1*, and *CTGF* (*CCN2*) were enriched in terms associated with integrins, such as integrin binding (GO: 0005178) in MF and integrin-mediated signaling pathway (GO: 0007229) in BP.

a



b

GO:MF

Term name	Term ID	p_{adj}
extracellular matrix structural constituent	GO:0005201	1.594×10^{-17}
structural molecule activity	GO:0005198	2.889×10^{-9}
extracellular matrix structural constituent conferring tensile ...	GO:0030020	1.513×10^{-6}
integrin binding	GO:0005178	3.332×10^{-4}
heparin binding	GO:0008201	5.162×10^{-4}

GO:BP

Term name	Term ID	p_{adj}
extracellular matrix organization	GO:0030198	1.835×10^{-7}
extracellular structure organization	GO:0043062	1.876×10^{-7}
external encapsulating structure organization	GO:0045229	1.959×10^{-7}
integrin-mediated signaling pathway	GO:0007229	5.017×10^{-6}
basement membrane organization	GO:0071711	5.538×10^{-6}
cell surface receptor signaling pathway	GO:0007166	1.164×10^{-4}
cellular response to amino acid stimulus	GO:0071230	1.519×10^{-4}
cellular response to acid chemical	GO:0071229	2.205×10^{-4}
cellular response to endogenous stimulus	GO:0071495	2.820×10^{-4}
cell adhesion	GO:0007155	3.588×10^{-4}
response to amino acid	GO:0043200	7.416×10^{-4}
response to endogenous stimulus	GO:0009719	9.080×10^{-4}

GO:CC

Term name	Term ID	p_{adj}
collagen-containing extracellular matrix	GO:0062023	1.302×10^{-16}
extracellular matrix	GO:0031012	2.829×10^{-15}
external encapsulating structure	GO:0030312	2.887×10^{-15}
basement membrane	GO:0005604	4.114×10^{-10}
endoplasmic reticulum lumen	GO:0005788	8.784×10^{-9}
extracellular region	GO:0005576	2.463×10^{-7}
collagen trimer	GO:0005581	1.560×10^{-5}
complex of collagen trimers	GO:0098644	1.780×10^{-5}
extracellular space	GO:0005615	2.830×10^{-5}
endomembrane system	GO:0012505	4.684×10^{-5}
cell periphery	GO:0071944	8.318×10^{-4}

Figure 4. GO analysis of 12 genes of Module A in g:Profiler. (**a**) Manhattan plot showing enriched terms of GO molecular functions (GO: MF), biological processes (GO: BP), or cellular components (GO: CC) in 12 genes. The black line indicates −log10(Padj) = 3. (**b**) Detailed results depicting 28 enriched terms with Padj < 0.001.

3.4. Selection and Analysis of Hub Genes

To identify hub genes in the PPI network identified, the 80 nodes were calculated using the MCC algorithm. The top 15 genes with high MCC scores were considered hub genes: *COL3A1*, *FBN1*, *COL4A1*, *COL5A2*, *POSTN*, *CTGF* (*CCN2*), *SPARC*, *HSPG2*, *FSTL1*, *LAMA2*, *LAMC1*, *COL16A1*, *SERPINE1*, *TAGLN*, and *SLCLA5* (Table 2). Interestingly, the top 12 of the 15 hub genes were identical to the 12 genes comprising Module A, suggesting that these 12 genes play crucial roles in the PPI network. The MCC scores of the remaining three genes, *SERPINE1*, *TAGLN*, and *SLCLA5*, were relatively low compared with those of the 12 genes. Notably, three of the top four genes were collagen genes: *COL3A1*, *COL4A1*, and *COL5A2*.

Table 2. Hub genes identified by MCC (Maximal Chique Centrality) algorithm.

	Gene Symbol	MCC Score	Module A	Fold Difference ± SD (AT-MSCs/FBs)
1	*COL3A1*	13,544	Yes	2.66 ± 1.34
2	*FBN1*	13,536	Yes	3.54 ± 1.93
3	*COL4A1*	13,232	Yes	5.57 ± 4.90
4	*COL5A2*	13,152	Yes	2.11 ± 0.23
5	*POSTN*	11,982	Yes	12.12 ± 15.05
6	*CTGF* (*CCN2*)	10,506	Yes	10.46 ± 6.42
7	*SPARC*	10,202	Yes	2.03 ± 0.42
8	*HSPG2*	6486	Yes	1.91 ± 0.26
9	*FSTL1*	5192	Yes	1.94 ± 0.09
10	*LAMA2*	2881	Yes	4.89 ± 3.11
11	*LAMC1*	1561	Yes	2.68 ± 0.39
12	*COL16A1*	1446	Yes	2.16 ± 0.41
13	*SERPINE1*	252	No	4.58 ± 1.53
14	*TAGLN*	243	No	3.13 ± 1.76
15	*SLC1A5*	82	No	2.18 ± 0.81

Module A indicates the significant module identified in this study (Figure 3b).

Next, we compared the expression levels of the 12 genes in AT-MSCs and FBs (Table 2). The expression levels of *POSTN* and *CTGF* in AT-MSCs were found to be at least 10-fold higher than those in FBs, suggesting that the genes in Module A may function as markers for distinguishing AT-MSCs from FBs.

4. Discussion

In this study, we compared MSCs and FBs, which share a high degree of similarity in terms of morphology and surface antigens at the molecular level. By analyzing 123 genes with higher expression levels in AT-MSCs compared to FBs, we constructed PPI networks and identified a module consisting of 12 genes (*COL3A1*, *FBN1*, *COL4A1*, *COL5A2*, *POSTN*, *CTGF*, *SPARC*, *HSPG2*, *FSTL1*, *LAMA2*, *LAMC1*, and *COL16A1*) (Module A). The MCC algorithm suggested that these 12 genes function as hub genes in the PPI network identified in this study.

Interestingly, *COL3A1* exhibited the highest MCC score among the 12 genes in Module A, suggesting that *COL3A1* may play a crucial role in maintaining the differentiation potential of MSCs. Type III collagen is primarily located in the medial layer of the arterial wall [33] and is also involved in the tenogenic differentiation ability of tendon stem/progenitor cells (TSPCs) [34]. Notably, the tenogenic differentiation ability of TSPCs derived from aged donors is significantly lower compared to those from young donors, with tendon-related markers, including *COL3A1*, being significantly downregulated in aged TSPCs [34]. Rong et al. also reported a significant decrease in *COL3A1* expression in senescent human MSCs [33]. *COL3A1* expression in senescent MSCs was restored by the overexpression of

the embryonic transcription factor *NANOG* [33], which was reported to be sufficient to reverse cellular aging and restore the differentiation ability of aged MSCs [35,36]. Together, these findings indicate that *COL3A1* may play an essential role in maintaining the differentiation ability of AT-MSCs. However, to date, knockdown or overexpression studies of *COL3A1* in AT-MSCs have not been reported, and such experiments will be necessary in the future to clarify its specific role in AT-MSC differentiation potentials.

Although *COL3A1* had the highest MCC score among the 12 genes (13,544), its expression ratio in AT-MSCs compared to FBs was ranked eighth (2.66-fold). In contrast, the expression ratios of *POSTN* and *CTGF* in AT-MSCs to FBs were both 10 times or higher, and the MCC scores of these two genes were also exceptionally high, exceeding 10,000. Furthermore, Ragelle et al. performed a proteomic characterization of extracellular matrices derived from AT-MSCs, BM-MSCs, and FBs and reported that high protein expression of CTGF and POSTN was detected in AT-MSC-derived matrices [25]. Given the expression ratios and MCC scores of *POSTN* and *CTGF*, they were considered effective markers. PPI network analysis also indicated strong associations between these two genes and the remaining ten genes in Module A. Therefore, we propose that these 12 genes could serve as gene markers for distinguishing AT-MSCs from FBs.

CTGF has been shown to regulate BM-MSC lineage fate through extracellular matrix interactions, particularly via modulation of the CTGF-VEGF complex by RhoA/ROCK signaling [37]. Activation of this pathway promotes myofibroblast differentiation of BM-MSC, whereas its inhibition facilitates endothelial differentiation. These findings suggest that CTGF functions as a key regulator of lineage specification, linking extracellular matrix cues to distinct differentiation outcomes in MSCs. Postn enhances AT-MSC adhesion, migration, and therapeutic efficiency in a murine ischemia model [38], and *POSTN* expression also decreases during adipogenic differentiation of AT-MSCs [39]. Together, these reports underscore the roles of CTGF and POSTN as ECM molecules influencing lineage specification, stemness, and regenerative capacity. However, despite these functional associations, experimental manipulation of *POSTN* expression in AT-MSCs has not been investigated, and further studies will be important to elucidate its precise function in stemness and differentiation.

In a previous study, we identified ten gene markers, including *CTGF*, for distinguishing between BM-MSCs and FBs [22]. The expression of *CTGF* in BM-MSCs was 15-fold higher than that in FBs. In the samples used in this study, the BM-MSC to FB expression ratio was 9.15-fold (Supplementary Table S3), while the ratio for AT-MSCs to FBs was 10.46-fold. Therefore, *CTGF* is considered a common marker of AT-MSCs and BM-MSCs.

GO analysis revealed that all 12 genes identified in this study were enriched in the extracellular region (GO:0005576). The extracellular matrix, which forms a stem cell niche, is essential for cell proliferation and differentiation [40]. Using LC-MS/MS, Soteriou et al. analyzed feeders for human embryonic stem (ES) cell culture and identified 42 extracellular proteins [41], 6 of which were encoded by the genes identified in this study: *COL3A1*, *FBN1*, *COL4A1*, *COL5A2*, *HSPG2*, and *LAMC1*. Interestingly, Soteriou et al. successfully cultured ES cells in dishes coated with fibrillin-1 (FBN1) alone or perlecan (HSPG2) in combination with fibronectin, without losing the undifferentiated characteristics of the cells. These findings suggest that some of the genes identified in this study play crucial roles in maintaining the stemness of both AT-MSCs and ES cells.

Our GO analysis also revealed that *COL3A1*, *COL16A1*, and *CTGF* (*CCN2*), identified in this study, were enriched in integrin-related terms such as integrin binding (GO:0005178) and the integrin-mediated signaling pathway (GO:0007229). Given that integrins play critical roles in stem cell functions [40], these findings suggest that *COL3A1*, *COL16A1*, and *CTGF* (*CCN2*), together with integrins, are involved in the stem cell characteristics

of AT-MSCs, including their high differentiation potential. Indeed, in a previous study, we identified the integrin subunit alpha 5 gene as a marker predicting the adipogenic differentiation potential of BM-MSCs [42], although no integrin gene was identified in this study.

As mentioned earlier, AT-MSCs cannot be easily distinguished from FBs based on phenotypic profiles, such as surface CD markers [14]. If AT-MSC cultures are contaminated with FBs, it becomes difficult to identify the contamination. Therefore, markers are required to distinguish between AT-MSCs and FBs. In the attempt to establish such markers, Melo et al. used RNA-seq and identified 910 genes highly expressed in AT-MSCs compared to FBs [43]. Similarly, Jääger et al. reported 59 genes more highly expressed in AT-MSCs than in FBs [44]. Among the 12 genes identified in this study, 9 genes were included in the list reported by Melo et al. [43]: *COL3A1*, *COL4A1*, *COL16A1*, *CTGF*, *FBN1*, *LAMA2*, *LAMC1*, *POSTN*, and *SPARC*. Additionally, the 59 genes reported by Jääger et al. contained 4 genes identified in this study: *COL3A1*, *COL16A1*, *POSTN*, and *SPARC*, all of which were included in the above 9 genes. These findings collectively suggest that these nine genes are particularly important for distinguishing AT-MSCs from FBs.

This study has several limitations. First, it relies on publicly available DNA microarray datasets rather than RNA-seq, which has recently become the mainstream approach for transcriptome analysis. Our laboratory has used DNA microarray platforms to study differences between MSCs and FBs, including BM-MSCs [22–24], even before RNA-seq became widely available. For this reason, we integrated array datasets from multiple laboratories to identify genes that consistently distinguish AT-MSCs from FBs across studies. Although RNA-seq could provide greater depth and resolution, we did not identify publicly available datasets containing matched samples of AT-MSCs, BM-MSCs, and FBs with sufficient replicates. Second, this study lacks experimental validation of the identified candidate genes. Future work should expand sample sizes and employ absolute quantification methods such as digital PCR to validate the expression levels of the 12 genes identified here. In addition, it will be important to correlate gene expression with AT-MSC differentiation capacity, to establish functional links between marker expression and cell fate.

5. Conclusions

In summary, hierarchical clustering analysis identified gene clusters that may distinguish AT-MSCs from FBs. In addition, we have identified a key module of 12 genes differentially expressed between AT-MSCs and FBs by constructing a PPI network. All 12 genes were enriched in the extracellular region categories, suggesting their involvement in the stem cell niche. Our findings suggest that these 12 genes could serve as markers to distinguish AT-MSCs from FBs and may play a role in maintaining the differentiation potential and stemness of AT-MSCs. These insights offer a novel approach for advancing regenerative medicine.

Supplementary Materials: The following supporting information can be downloaded at https://www.mdpi.com/article/10.3390/app15189881/s1: Table S1: Differentially expressed 123 genes between AT-MSCs and FBs among 3 studies. Table S2: GO analysis for Module A. Table S3: Differentially expressed 96 genes between BM-MSCs and FBs among 3 studies.

Author Contributions: M.K. conducted the research, while M.K. and T.K. were responsible for drafting the manuscript. K.F. and A.N. were involved in the study's conception and design. M.K., T.K., and T.S. took part in revising and editing the manuscript. They all agreed to accept responsibility and accountability for the article's content and to collectively address any inquiries regarding the accuracy or integrity of the published work. All authors have read and agreed to the published version of the manuscript.

Funding: This work was supported by JSPS KAKENHI Grant Number JP21K097920A.

Institutional Review Board Statement: Not applicable.

Informed Consent Statement: Not applicable.

Data Availability Statement: The datasets analyzed in the study could be found in the GEO portal (https://www.ncbi.nlm.nih.gov/geo/ (accessed on 24 May 2022)).

Conflicts of Interest: The authors declare no conflicts of interest.

Abbreviations

The following abbreviations are used in this manuscript:

AT-MSCs	Adipose-derived Mesenchymal Stromal/Stem Cells
BM-MSCs	Bone Marrow-derived Mesenchymal Stromal/Stem Cells
DEGs	Differentially Expressed Genes
ES Cells	Embryonic Stem Cells
FBs	Fibroblasts
GO	Gene Ontology
GEO	Gene Expression Omnibus
MCC	Maximal Clique Centrality
MCODE	Molecular Complex Detection

References

1. Pittenger, M.F.; Mackay, A.M.; Beck, S.C.; Jaiswal, R.K.; Douglas, R.; Mosca, J.D.; Moorman, M.A.; Simonetti, D.W.; Craig, S.; Marshak, D.R. Multilineage potential of adult human mesenchymal stem cells. *Science* **1999**, *284*, 143–147. [CrossRef]
2. Liu, Y.; Yang, Z.; Na, J.; Chen, X.; Wang, Z.; Zheng, L.; Fan, Y. In vitro stretch modulates mitochondrial dynamics and energy metabolism to induce smooth muscle differentiation in mesenchymal stem cells. *FASEB J.* **2025**, *39*, e70354. [CrossRef] [PubMed]
3. Tropel, P.; Platet, N.; Platel, J.C.; Noel, D.; Albrieux, M.; Benabid, A.L.; Berger, F. Functional neuronal differentiation of bone marrow-derived mesenchymal stem cells. *Stem Cells* **2006**, *24*, 2868–2876. [CrossRef]
4. Beeravolu, N.; McKee, C.; Alamri, A.; Mikhael, S.; Brown, C.; Perez-Cruet, M.; Chaudhry, G.R. Isolation and Characterization of Mesenchymal Stromal Cells from Human Umbilical Cord and Fetal Placenta. *J. Vis. Exp.* **2017**, *2017*, e55224. [CrossRef] [PubMed]
5. Xu, X.; Xu, L.; Xia, J.; Wen, C.; Liang, Y.; Zhang, Y. Harnessing knee joint resident mesenchymal stem cells in cartilage tissue engineering. *Acta Biomater.* **2023**, *168*, 372–387. [CrossRef]
6. Fujii, S.; Fujimoto, K.; Goto, N.; Abiko, Y.; Imaoka, A.; Shao, J.; Kitayama, K.; Kanawa, M.; Sosiawan, A.; Suardita, K.; et al. Characterization of human dental pulp cells grown in chemically defined Serum-Free medium. *Biomed. Rep.* **2018**, *8*, 350–358. [CrossRef]
7. Hemmingsen, M.; Vedel, S.; Skafte-Pedersen, P.; Sabourin, D.; Collas, P.; Bruus, H.; Dufva, M. The role of paracrine and autocrine signaling in the early phase of adipogenic differentiation of adipose-derived stem cells. *PLoS ONE* **2013**, *8*, e63638. [CrossRef]
8. Choudhery, M.S.; Badowski, M.; Muise, A.; Pierce, J.; Harris, D.T. Subcutaneous Adipose Tissue-Derived Stem Cell Utility Is Independent of Anatomical Harvest Site. *Biores. Open Access* **2015**, *4*, 131–145. [CrossRef] [PubMed]
9. Oedayrajsingh-Varma, M.J.; van Ham, S.M.; Knippenberg, M.; Helder, M.N.; Klein-Nulend, J.; Schouten, T.E.; Ritt, M.J.P.F.; van Milligen, F.J. Adipose tissue-derived mesenchymal stem cell yield and growth characteristics are affected by the tissue-harvesting procedure. *Cytotherapy* **2006**, *8*, 166–177. [CrossRef]
10. Kanawa, M.; Igarashi, A.; Fujimoto, K.; Saskianti, T.; Nakashima, A.; Higashi, Y.; Kurihara, H.; Kato, Y.; Kawamoto, T. The Identification of Marker Genes for Predicting the Osteogenic Differentiation Potential of Mesenchymal Stromal Cells. *Curr. Issues Mol. Biol.* **2021**, *43*, 2157–2166. [CrossRef]
11. Pereira, M.C.L.; Secco, M.; Suzuki, D.E.; Janjoppi, L.; Rodini, C.O.; Torres, L.B.; Araújo, B.H.S.; Cavalheiro, E.A.; Zatz, M.; Okamoto, O.K. Contamination of Mesenchymal Stem-Cells with Fibroblasts Accelerates Neurodegeneration in an Experimental Model of Parkinson's Disease. *Stem Cell Rev. Rep.* **2011**, *7*, 1006–1017. [CrossRef]
12. Dominici, M.; Le Blanc, K.; Mueller, I.; Slaper-Cortenbach, I.; Marini, F.; Krause, D.; Deans, R.; Keating, A.; Prockop, D.; Horwitz, E. Minimal criteria for defining multipotent mesenchymal stromal cells. The International Society for Cellular Therapy position statement. *Cytotherapy* **2006**, *8*, 315–317. [CrossRef]
13. Alt, E.; Yan, Y.; Gehmert, S.; Song, Y.-H.; Altman, A.; Gehmert, S.; Vykoukal, D.; Bai, X. Fibroblasts share mesenchymal phenotypes with stem cells, but lack their differentiation and colony-forming potential. *Biol. Cell* **2011**, *103*, 197–208. [CrossRef]

14. Zanata, F.; Curley, L.; Martin, E.; Bowles, A.; Bunnell, B.A.; Wu, X.; Ferreira, L.M.; Gimble, J.M. Comparative Analysis of Human Adipose-Derived Stromal/Stem Cells and Dermal Fibroblasts. *Stem Cells Dev.* **2021**, *30*, 1171–1178. [CrossRef]
15. Shen, S.; Kong, J.; Qiu, Y.; Yang, X.; Wang, W.; Yan, L. Identification of core genes and outcomes in hepatocellular carcinoma by bioinformatics analysis. *J. Cell Biochem.* **2019**, *120*, 10069–10081. [CrossRef]
16. Yang, H.; Wu, J.; Zhang, J.; Yang, Z.; Jin, W.; Li, Y.; Jin, L.; Yin, L.; Liu, H.; Wang, Z. Integrated bioinformatics analysis of key genes involved in progress of colon cancer. *Mol. Genet. Genomic Med.* **2019**, *7*, e00588. [CrossRef] [PubMed]
17. Zeng, X.; Shi, G.; He, Q.; Zhu, P. Screening and predicted value of potential biomarkers for breast cancer using bioinformatics analysis. *Sci. Rep.* **2021**, *11*, 20799. [CrossRef]
18. Ma, H.; He, Z.; Chen, J.; Zhang, X.; Song, P. Identifying of biomarkers associated with gastric cancer based on 11 topological analysis methods of CytoHubba. *Sci. Rep.* **2021**, *11*, 1331. [CrossRef] [PubMed]
19. Yin, X.; Wu, Q.; Hao, Z.; Chen, L. Identification of novel prognostic targets in glioblastoma using bioinformatics analysis. *Biomed. Eng. Online* **2022**, *21*, 26. [CrossRef] [PubMed]
20. Zhao, X.; Liang, M.; Li, X.; Qiu, X.; Cui, L. Identification of key genes and pathways associated with osteogenic differentiation of adipose stem cells. *J. Cell Physiol.* **2018**, *233*, 9777–9785. [CrossRef]
21. Liang, T.; Li, P.; Liang, A.; Zhu, Y.; Qiu, X.; Qiu, J.; Peng, Y.; Huang, D.; Gao, W.; Gao, B. Identifying the key genes regulating mesenchymal stem cells chondrogenic differentiation: An in vitro study. *BMC Musculoskelet. Disord.* **2022**, *23*, 985. [CrossRef]
22. Igarashi, A.; Segoshi, K.; Sakai, Y.; Pan, H.; Kanawa, M.; Higashi, Y.; Sugiyama, M.; Nakamura, K.; Kurihara, H.; Yamaguchi, S.; et al. Selection of common markers for bone marrow stromal cells from various bones using real-time RT-PCR: Effects of passage number and donor age. *Tissue Eng.* **2007**, *13*, 2405–2417. [CrossRef]
23. Kubo, H.; Shimizu, M.; Taya, Y.; Kawamoto, T.; Michida, M.; Kaneko, E.; Igarashi, A.; Nishimura, M.; Segoshi, K.; Shimazu, Y.; et al. Identification of mesenchymal stem cell (MSC)-transcription factors by microarray and knockdown analyses, and signature molecule-marked MSC in bone marrow by immunohistochemistry. *Genes. Cells* **2009**, *14*, 407–424. [CrossRef]
24. Fujii, S.; Fujimoto, K.; Goto, N.; Kanawa, M.; Kawamoto, T.; Pan, H.; Srivatanakul, P.; Rakdang, W.; Pornprasitwech, J.; Saskianti, T.; et al. Characteristic expression of MSX1, MSX2, TBX2 and ENTPD1 in dental pulp cells. *Biomed. Rep.* **2015**, *3*, 566–572. [CrossRef]
25. Ragelle, H.; Naba, A.; Larson, B.L.; Zhou, F.; Prijić, M.; Whittaker, C.A.; Del Rosario, A.; Langer, R.; Hynes, R.O.; Anderson, D.G. Comprehensive proteomic characterization of stem cell-derived extracellular matrices. *Biomaterials* **2017**, *128*, 147–159. [CrossRef] [PubMed]
26. Lim, M.N. Comparative Gene Expression Profile of Human Limbal Stromal Cells, Bone Marrow Mesenchymal Cells, Adipose Cells and Foreskin Fibroblasts. 2014. Available online: https://www.ncbi.nlm.nih.gov/geo/query/acc.cgi?acc=GSE38947/ (accessed on 7 September 2025).
27. Szklarczyk, D.; Morris, J.H.; Cook, H.; Kuhn, M.; Wyder, S.; Simonovic, M.; Santos, A.; Doncheva, N.T.; Roth, A.; Bork, P.; et al. The STRING database in 2017: Quality-controlled protein-protein association networks, made broadly accessible. *Nucleic Acids Res.* **2017**, *45*, D362–D368. [CrossRef] [PubMed]
28. Szklarczyk, D.; Kirsch, R.; Koutrouli, M.; Nastou, K.; Mehryary, F.; Hachilif, R.; Gable, A.L.; Fang, T.; Doncheva, N.T.; Pyysalo, S.; et al. The STRING database in 2023: Protein-protein association networks and functional enrichment analyses for any sequenced genome of interest. *Nucleic Acids Res.* **2023**, *51*, D638–D646. [CrossRef] [PubMed]
29. Shannon, P.; Markiel, A.; Ozier, O.; Baliga, N.S.; Wang, J.T.; Ramage, D.; Amin, N.; Schwikowski, B.; Ideker, T. Cytoscape: A software environment for integrated models of biomolecular interaction networks. *Genome Res.* **2003**, *13*, 2498–2504. [CrossRef]
30. Bader, G.D.; Hogue, C.W. An automated method for finding molecular complexes in large protein interaction networks. *BMC Bioinform.* **2003**, *4*, 2. [CrossRef]
31. Chin, C.H.; Chen, S.H.; Wu, H.H.; Ho, C.W.; Ko, M.T.; Lin, C.Y. cytoHubba: Identifying hub objects and sub-networks from complex interactome. *BMC Syst. Biol.* **2014**, *8* (Suppl. S4), S11. [CrossRef]
32. Raudvere, U.; Kolberg, L.; Kuzmin, I.; Arak, T.; Adler, P.; Peterson, H.; Vilo, J. G:Profiler: A web server for functional enrichment analysis and conversions of gene lists (2019 update). *Nucleic Acids Res.* **2019**, *47*, W191–W198. [CrossRef]
33. Rong, N.; Mistriotis, P.; Wang, X.; Tseropoulos, G.; Rajabian, N.; Zhang, Y.; Wang, J.; Liu, S.; Andreadis, S.T. Restoring extracellular matrix synthesis in senescent stem cells. *FASEB J.* **2019**, *33*, 10954–10965. [CrossRef]
34. Han, W.; Wang, B.; Liu, J.; Chen, L. The p16/miR-217/EGR1 pathway modulates age-related tenogenic differentiation in tendon stem/progenitor cells. *Acta Biochim. Biophys. Sin.* **2017**, *49*, 1015–1021. [CrossRef] [PubMed]
35. Mistriotis, P.; Andreadis, S.T. Vascular aging: Molecular mechanisms and potential treatments for vascular rejuvenation. *Ageing Res. Rev.* **2017**, *37*, 94–116. [CrossRef] [PubMed]
36. Shahini, A.; Mistriotis, P.; Asmani, M.; Zhao, R.; Andreadis, S.T. NANOG Restores Contractility of Mesenchymal Stem Cell-Based Senescent Microtissues. *Tissue Eng. Part. A* **2017**, *23*, 535–545. [CrossRef]
37. Li, C.; Zhen, G.; Chai, Y.; Xie, L.; Crane, J.L.; Farber, E.; Farber, C.R.; Luo, X.; Gao, P.; Cao, X.; et al. RhoA determines lineage fate of mesenchymal stem cells by modulating CTGF-VEGF complex in extracellular matrix. *Nat. Commun.* **2016**, *7*, 11455. [CrossRef]

38. Qin, J.; Yuan, F.; Peng, Z.; Ye, K.; Yang, X.; Huang, L.; Jiang, M.; Lu, X. Periostin enhances adipose-derived stem cell adhesion, migration, and therapeutic efficiency in Apo E deficient mice with hind limb ischemia. *Stem Cell Res. Ther.* **2015**, *6*, 138. [CrossRef]
39. Satish, L.; Krill-Burger, J.M.; Gallo, P.H.; Etages, S.D.; Liu, F.; Philips, B.J.; Ravuri, S.; Marra, K.G.; LaFramboise, W.A.; Kathju, S.; et al. Expression analysis of human adipose-derived stem cells during in vitro differentiation to an adipocyte lineage. *BMC Med. Genomics* **2015**, *8*, 41. [CrossRef]
40. Novoseletskaya, E.S.; Evdokimov, P.V.; Efimenko, A.Y. Extracellular matrix-induced signaling pathways in mesenchymal stem/stromal cells. *Cell Commun. Signal* **2023**, *21*, 244. [CrossRef]
41. Soteriou, D.; Iskender, B.; Byron, A.; Humphries, J.D.; Borg-Bartolo, S.; Haddock, M.C.; Baxter, M.A.; Knight, D.; Humphries, M.J.; Kimber, S.J. Comparative proteomic analysis of supportive and unsupportive extracellular matrix substrates for human embryonic stem cell maintenance. *J. Biol. Chem.* **2013**, *288*, 18716–18731. [CrossRef] [PubMed]
42. Kanawa, M.; Igarashi, A.; Fujimoto, K.; Ronald, V.S.; Higashi, Y.; Kurihara, H.; Kato, Y.; Kawamoto, T. Potential Marker Genes for Predicting Adipogenic Differentiation of Mesenchymal Stromal Cells. *Appl. Sci.* **2019**, *9*, 2942. [CrossRef]
43. Abreu de Melo, M.I.; da Silva Cunha, P.; Coutinho de Miranda, M.; Faraco, C.C.F.; Barbosa, J.L.; da Fonseca Ferreira, A.; Kunrath Lima, M.; Faria, J.A.Q.A.; Rodrigues, M.Â.; de Goes, A.M.; et al. Human adipose-derived stromal/stem cells are distinct from dermal fibroblasts as evaluated by biological characterization and RNA sequencing. *Cell Biochem. Funct.* **2021**, *39*, 442–454. [CrossRef] [PubMed]
44. Jaager, K.; Islam, S.; Zajac, P.; Linnarsson, S.; Neuman, T. RNA-seq analysis reveals different dynamics of differentiation of human dermis- and adipose-derived stromal stem cells. *PLoS ONE* **2012**, *7*, e38833. [CrossRef] [PubMed]

Disclaimer/Publisher's Note: The statements, opinions and data contained in all publications are solely those of the individual author(s) and contributor(s) and not of MDPI and/or the editor(s). MDPI and/or the editor(s) disclaim responsibility for any injury to people or property resulting from any ideas, methods, instructions or products referred to in the content.